ORIGINAL PAPER

RJME
Romanian Journal of Morphology & Embryology
http://www.rjme.ro/

Study of antimicrobial effects of functionalized silver nanoparticles

ELENA LEOCADIA POPESCU[1)], MARIA BĂLĂŞOIU[2)], OANA MARIANA CRISTEA[2)], ALEXANDRA ELENA STOICA[3)], OVIDIU CRISTIAN OPREA[4)], BOGDAN ŞTEFAN VASILE[3)], ALEXANDRU MIHAI GRUMEZESCU[3)], GABRIELA BĂNCESCU[5)], CRISTINA JANA BUSUIOC[6)], GEORGE DAN MOGOŞANU[7)], COSTIN TEODOR STREBA[8)], LAURENŢIU MOGOANTĂ[6)]

[1)]*Doctoral School, University of Medicine and Pharmacy of Craiova, Romania*

[2)]*Department of Microbiology, University of Medicine and Pharmacy of Craiova, Romania*

[3)]*Department of Science and Engineering of Oxide Materials and Nanomaterials, Faculty of Applied Chemistry and Materials Science, Politehnica University of Bucharest, Romania*

[4)]*Department of Inorganic Chemistry, Physical Chemistry and Electrochemistry, Politehnica University of Bucharest, Romania*

[5)]*Department of Microbiology, Faculty of Dental Medicine, "Carol Davila" University of Medicine and Pharmacy, Bucharest, Romania*

[6)]*Department of Histology, University of Medicine and Pharmacy of Craiova, Romania*

[7)]*Department of Pharmacognosy & Phytotherapy, Faculty of Pharmacy, University of Medicine and Pharmacy of Craiova, Romania*

[8)]*Department of Research Methodology, University of Medicine and Pharmacy of Craiova, Romania*

Abstract

In recent decades, the study of nanoparticles (NPs) has gained a great scientific interest, due to a wide range of potential applications, in different fields: electronic, optical and biomedical. Some of the most studied effects of NPs are antibacterial ones, because the large, sometimes unjustified and uncontrolled administration of antibiotics has led to the emergence of multidrug-resistant (MDR) bacterial strains. In our study, starting from silver nitrate ($AgNO_3$), we made approximately 30 nm spherical AgNPs that were coated with a thin layer of ethylene glycol (EG) or EG and polyvinylpyrrolidone (PVP). The microbial culture study showed that AgNPs have antibacterial effects, depending on the dose of the NPs and the type of bacteria.

Keywords: multidrug resistance, antibiotics, silver nanoparticles, antibacterial agent.

Introduction

Despite the fact that the emergence of antibiotic drugs has been a huge step forward for the medical world regarding the treatment of many infectious diseases, the resistance acquired by some pathogens to antibiotics represents a major public health concern for medical systems throughout the world [1–4].

Administration of broad-spectrum antibiotics or their use in different combinations resulted in the emergence of multidrug resistant (MDR) or pan-resistant bacterial strains. Thus, the increasing number of community or nosocomial infections due to MDR pathogens for which there is no effective antibiotic treatment is becoming an increasingly difficult obstacle to overcome [5–7].

To this date, an effective way to combat this phenomenon has not yet been discovered, apart from modifying the set of medicines administered or using stronger active substances to prevent the development of biofilms, the natural survival structures of bacteria.

In recent years, several studies have been focusing their attention on the emerging nanotechnologies that use functionalized nanoparticles (NPs) as a viable alternative for antibiotic drugs [8–13]. Among the many types of NPs, a special interest was given to silver nanoparticles (AgNPs) [14–18]. AgNPs have increased interest in various medical applications, after it has been found that they have a high capacity to inhibit many types of pathogenic bacteria, have anti-inflammatory and even anti-tumor activity [19–26]. Research over the past 20 years has led to the hypothesis that AgNPs could be a new class of antibiotics that act against a large number of pathogens, including those that have developed antibiotic resistance [27, 28].

Aim

The present study aims to evaluate the bactericidal/bacteriostatic action of two types of AgNPs: ethylene glycol (EG) functionalized AgNPs (Ag/EG) and EG and polyvinylpyrrolidone (PVP) functionalized AgNPs (Ag/EG/PVP), on several pathogenic bacteria.

Materials and Methods

Obtaining of AgNPs

Materials

All chemicals used in the experiments were of analytical reagent grade and were used without further purification.

Preparation of functionalized AgNPs

Functionalized AgNPs (Ag/EG and Ag/EG/PVP) were prepared by a reduction reaction from silver nitrate ($AgNO_3$), in alkaline solution, as follows: 0.1 g of $AgNO_3$ was dissolved in 100 mL of distilled water under stirring. The reducing solution was prepared by dissolving 1 mL of EG and 4 g of sodium hydroxide in 300 mL of distilled water. Subsequently, the first solution was slowly dropped over the second solution, at 70°C, under stirring conditions, resulting in a brown dispersion. In the end, AgNPs (Ag/EG) were washed several times by centrifugation and dried at room temperature. In the case of Ag/EG/PVP, preparation procedure was similar with Ag/EG, with some minor improvements: 1 g of PVP were added in the reducing solution.

Characterization methods

Transmission electron microscopy (TEM)

TEM was done using a Tecnai™ G2 F30 S-TWIN high resolution (HR)-TEM (FEI Company, Hillsboro, OR, USA) equipment with selected area electron diffraction (SAED). The samples preparation steps consisted in dispersing the powders in ethanol, followed by sonication during 15 minutes and successive dilutions of the resulted suspensions, in order to result low concentrations suitable for the analysis. The following step consisted in placing the suspension onto a holey carbon–copper grid and drying. The equipment was set to transmission mode at 300 kV, with 2 Å point resolution and 1 Å line resolution.

Differential thermal analysis–Thermogravimetry (DTA–TG)

DTA–TG analysis was performed by DSC Jupiter, STA 449C (Netzsch, Germany) equipment. The samples (10 mg) were weighed directly in a standard alumina pan. An empty alumina pan was used as reference. The samples were heated from 25°C to 900°C, at a scanning rate of 10°C/min.

Fourier-transform infrared (FTIR) spectroscopy

IR analysis was performed on a Thermo Scientific Nicolet iS50 FTIR spectrometer (Thermo Fischer Scientific, Waltham, MA, USA). Thirty-two individual scans were recorded for each sample between 4000 and 400 cm^{-1} wavenumbers, at 4 cm^{-1} resolution, co-added and converted to absorbance spectra by using the OMNIC™ software package.

Microbiological testing

Bacterial strains

The bacterial strains tested were:

[I] Reference strains [in conformity with the Clinical & Laboratory Standards Institute (CLSI)/European Committee on Antimicrobial Susceptibility Testing (EUCAST)] whose sensitivity was known (Figure 1):

- *Staphylococcus aureus* American Type Culture Collection (ATCC) 25923 β-lactamase negative strain;
- *Escherichia coli* ATCC 25922 β-lactamase negative strain;
- *Pseudomonas aeruginosa* ATCC 27853 extended-spectrum β-lactamases (ESBL) negative strain;
- *Candida albicans* ATCC 10231 strain.

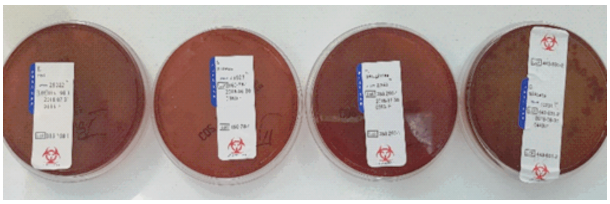

Figure 1 – ***The four microbial reference strains. From left to right:*** **E. coli** ***ATCC 25922,*** **S. aureus** ***ATCC 25923,*** **P. aeruginosa** ***ATCC 27853 and*** **C. albicans** ***ATCC 10231.***

[II] Antibiotic resistant (MDR) strains, represented by:

- Multidrug-resistant *S. aureus* (MRSA) resistant to β-lactam antibiotics, isolated from a patient's sputum;
- *E. coli* resistant to β-lactam antibiotics, aminoglycosides, fluoroquinolones, isolated from a tracheobronchial secretion;
- *P. aeruginosa* sensitive only to Colistin, isolated from the urine of a patient through uroculture;
- *C. albicans* isolated from a patient's pharyngeal exudate, resistant to Fluconazole, Voriconazole, Miconazole, Caspofungin, Flucytosine and Amphotericin B.

Diffusimetric method

For the diffusimetric method, sterile microdisks (blanks) were used, which were then impregnated with the AgNPs functionalized with EG (Ag/EG) and with EG and PVP (Ag/EG/PVP). These had an initial concentration of 1 mg/mL, at neutral pH, from which binary dilutions (1/1, 1/2, 1/4, 1/8, 1/16, 1/32) were performed. The amount of AgNPs solution that impregnated each microdisk was 35 µg.

Each bacterial strain to be tested was resuspended in liquid broth medium and checked to 0.5 McFarland turbidimetric standard, which corresponds to a density of 10^8 colony-forming units (CFU)/mL. The tested strains were then seeded on a Müller–Hinton solid-agar medium, poured into Petri dishes. After 20 minutes, during which the bacterial culture was impregnated in the solid culture medium, microdisks containing the two types of AgNPs (Ag/EG and Ag/EG/PVP) were applied on the surface of the Petri dishes, with a pin, under aseptic conditions, leaving a distance of 30 mm between them and 15 mm from the edge of the plate. For the *S. aureus* ATCC 25923 β-lactamase negative strain, microdisks were impregnated with two types of AgNPs in 1/1, 1/2, 1/4, 1/8, 1/16 and 1/32 dilutions.

Petri dishes were then incubated at 37°C for 18–24 hours. In the end, the diameter of the inhibition zones produced by each type of AgNPs that were impregnated on the sterile microdisks was measured for all of the tested microbial strains. Also, in the case of the *S. aureus* ATCC 25923 β-lactamase-negative strain, measurements were made for each dilution separately.

Control of media and antibacterial substances was done using a microdisk that was not impregnated or was impregnated with saline (negative control), and with a microdisk impregnated with a chemotherapeutic agent with known concentration from the CLSI/EUCAST standard (positive control).

The results were quantified and analyzed using the Microsoft Office 2010 Excel software package and the AnalysisPro (image analysis) software.

Results

Characterization of AgNPs by TEM

Prepared samples, Ag/EG and Ag/EG/PVP NPs were characterized by TEM. The main results are plotted in Figure 2 (a–c) for Ag/EG NPs and in Figure 3 (a–c) for Ag/EG/PVP NPs. As it can be seen in Figures 2a and 3a, SAED pattern confirm that the unique crystalline phase presented in the samples is assigned to the AgNPs. In the Figure 2 (b and c) are presented TEM and HR-TEM images that highlight the crystalline shape of functionalized AgNPs. According to the TEM images, the dimension of Ag/EG NPs did not exceed 30 nm. Similarly, TEM images of Ag/EG/PVP NPs present the same characteristics.

DTA–TG analysis

Thermal analysis allowed the estimation of the amount of monomer (EG)/polymer (PVP) interacting with Ag NPs (Figure 4, a and b).

In the case of Ag/EG, mass loss up to 215°C is 1.33%. The process is accompanied by an endothermic effect, at 194.9°C, caused by EG evaporation from the outer layers, which is not attached to the surface of the NPs [EG has a boiling point (b.p.) of 197.3°C].

Mass loss continues slowly to 340°C (-1.25%), with more strongly linked EG molecules. The main stage of sample decomposition is between 340–420°C, when a 12.95% loss occurs, the process being accompanied by a sharp endothermic effect with a minimum of 385.2°C. Whether it is a decomposition of EG linked to AgNPs, or there breaks the EG–Ag bonds and EG is also completely volatilized. The residual mass is 84.28%.

In case of Ag/EG/PVP sample, the thermal analysis in the first phase is similar. Mass loss up to 210°C is 2.49%, with an endothermic effect at 193.5°C, probably due to the evaporation of a portion of EG. Then, there is a mass loss of 6.59% up to 290°C, accompanied by an endothermic effect with a minimum of 256.1°C. The two processes are superimposed and although we see them separately on the differential scanning calorimetry (DSC), the TG curve forms a single stage of mass loss. Between 290–420°C, the sample loses 6.14%, the process being also an endothermic one, the effect having a minimum of 393.8°C. The residual mass has 84.57%.

FTIR spectroscopy

The obtained samples were characterized by FTIR spectroscopy. The results obtained are shown in Figure 5. It can be seen the absorption bands characteristic of EG. PVP could not be identified in the FTIR recorded spectra because the amount of PVP that has interacted with AgNPs is below 3%, this amount of PVP being below of the limit detection of the equipment. Under these conditions, the absorption bands identified are: the absorption band at 1068 cm^{-1}, characteristic of the C–O–H group; the absorption bands at 1324 cm^{-1} and 1399 cm^{-1}, characteristic of the deformation C–H groups. Also, the absorption bands characteristic of the C–H stretching were identified at 2853 cm^{-1} and 2922 cm^{-1}.

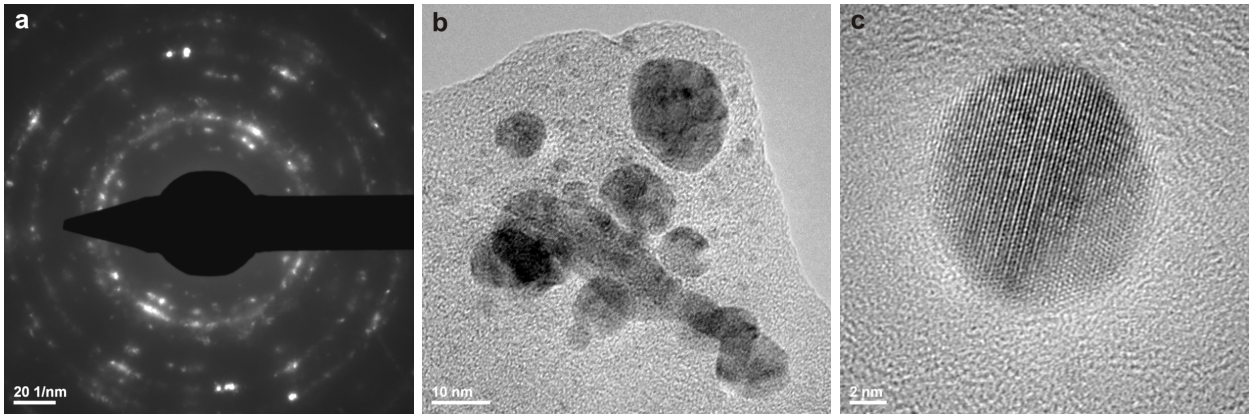

Figure 2 – ***SAED pattern (a) and TEM images (b and c) of AgNPs functionalized with EG (Ag/EG). SAED: Selected area electron diffraction; TEM: Transmission electron microscopy; AgNPs: Silver nanoparticles; EG: Ethylene glycol.***

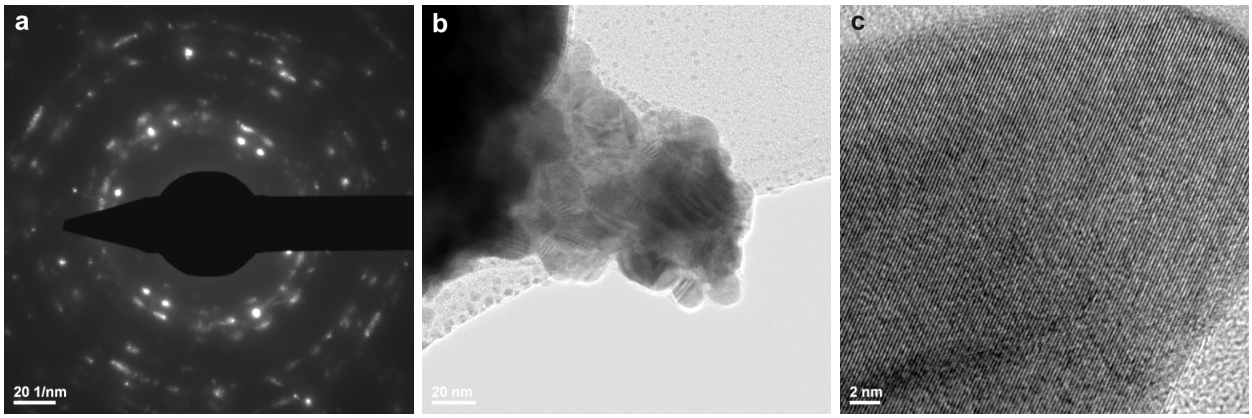

Figure 3 – ***SAED pattern (a) and TEM images (b and c) of AgNPs functionalized with EG and PVP (Ag/EG/PVP). SAED: Selected area electron diffraction; TEM: Transmission electron microscopy; AgNPs: Silver nanoparticles; EG: Ethylene glycol; PVP: Polyvinylpyrrolidone.***

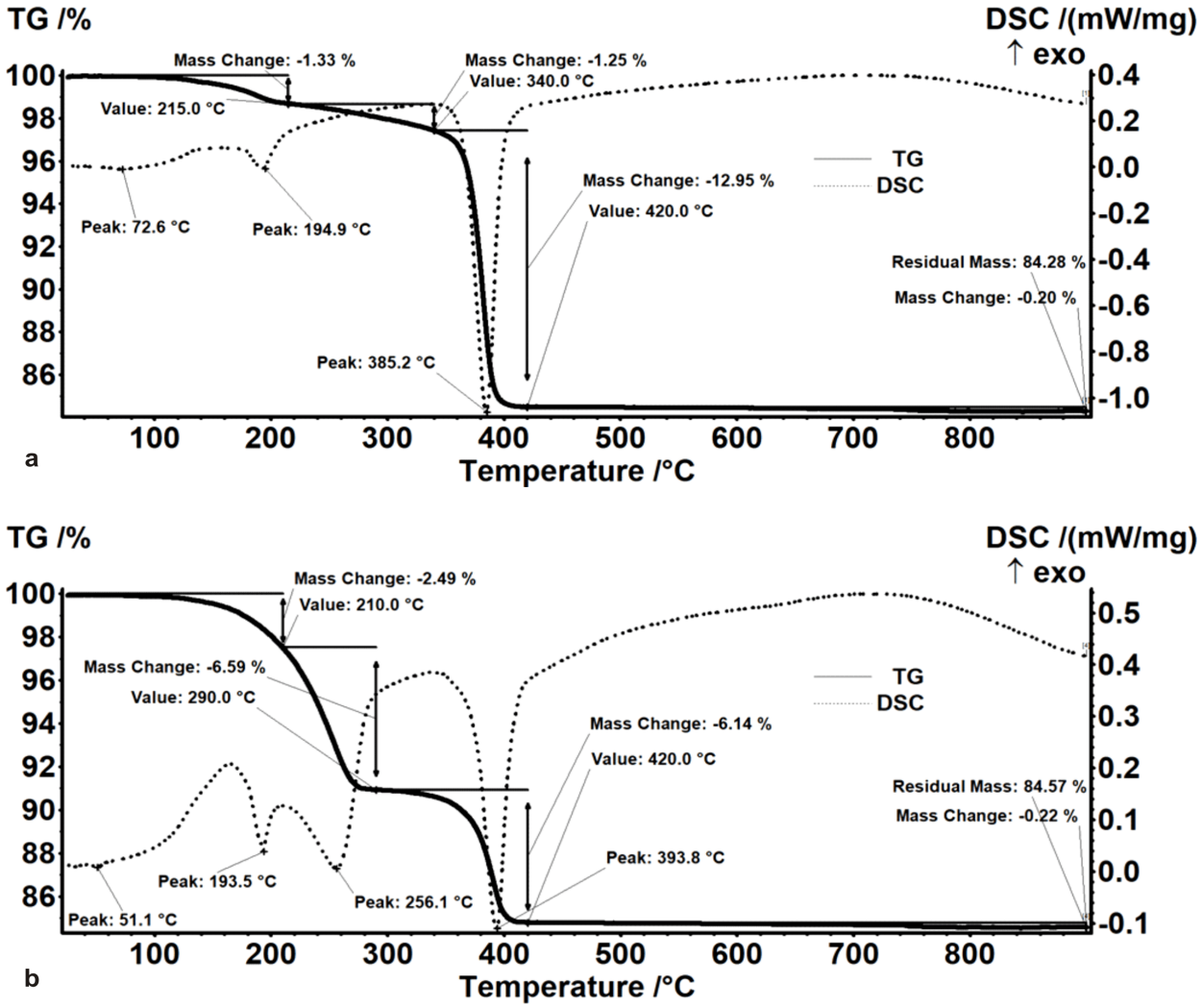

Figure 4 – ***DTA–TG analyses for Ag/EG NPs (a) and Ag/EG/PVP NPs (b). DTA–TG: Differential thermal analysis–Thermogravimetry; DSC: Differential scanning calorimetry; Ag: Silver; EG: Ethylene glycol; PVP: Polyvinylpyrrolidone; NPs: Nanoparticles.***

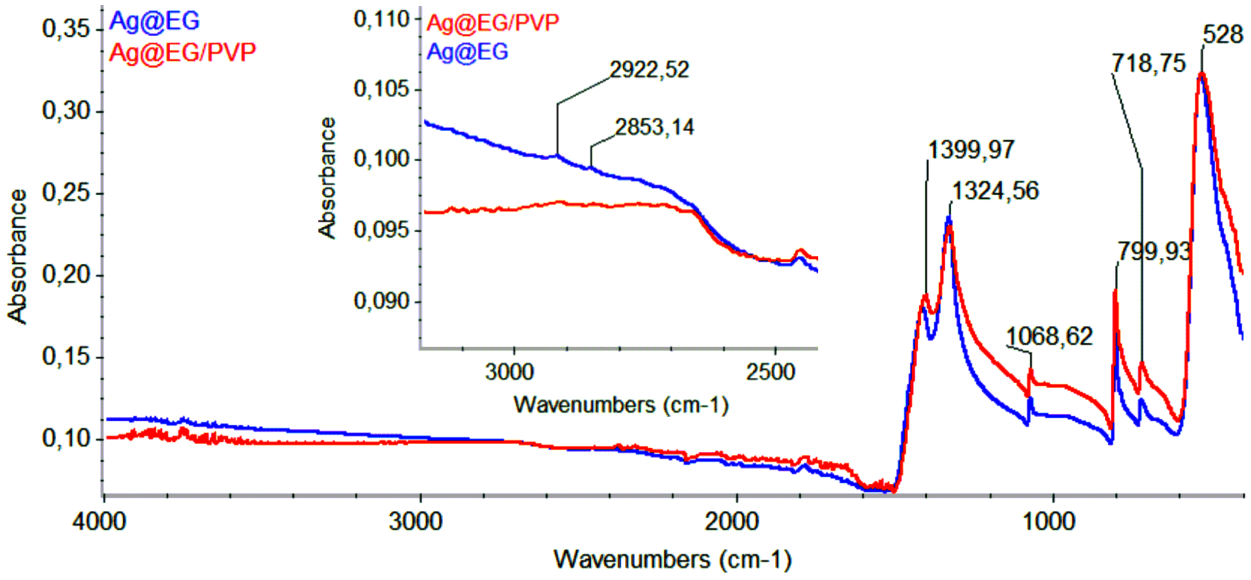

Figure 5 – ***FTIR spectra for Ag/EG NPs and Ag/EG/PVP NPs. FTIR: Fourier-transform infrared; Ag: Silver; EG: Ethylene glycol; PVP: Polyvinylpyrrolidone; NPs: Nanoparticles.***

Results of the microbiological assay

Following testing using the diffusimetric method and the evaluation of the inhibition zones (halos) that appeared around the microdisks impregnated with the two types of AgNPs, in an amount of 35 μg, the following evolutions could be observed:

Ag/EG NPs formed the largest inhibition zone on the *C. albicans* ATCC 10231 strain, having a diameter of 13.27 mm and an area of 138.2 mm^2. This was followed by the *S. aureus* ATCC 25923 strain, where the inhibition zone had a diameter of 9.48 mm and an area of 70.55 mm^2 (Figure 6a), and by the *P. aeruginosa* ATCC 27853 strain, that had an inhibition zone with a diameter of 9.29 mm and an area of 67.75 mm^2. For the *E. coli* ATCC 25922 strain, the diameter of the inhibition zone was 8.17 mm, and its area measured approximately 52.4 mm^2 (Table 1).

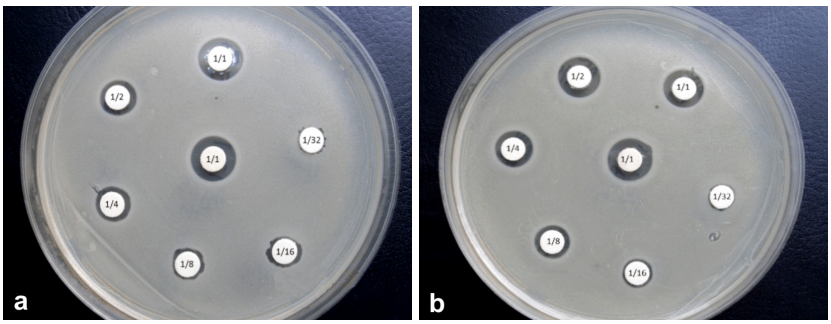

Figure 6 – ***Bacteriostatic effect of Ag/EG NPs (a) and Ag/EG/PVP NPs (b) against*** **S. aureus** ***ATCC 25923 reference strain. Ag: Silver; EG: Ethylene glycol; PVP: Polyvinylpyrrolidone; NPs: Nanoparticles; ATCC: American Type Culture Collection.***

Table 1 – ***Diameter and area of the inhibition zone developed by Ag/EG NPs against the four microbial reference strains***

Reference strain	Diameter of the inhibition zone [mm]	Area of the inhibition zone [mm^2]
S. aureus ATCC 25923	9.48	70.55
E. coli ATCC 25922	8.17	52.4
P. aeruginosa ATCC 27853	9.29	67.75
C. albicans ATCC 10231	13.27	138.2

Ag: Silver; EG: Ethylene glycol; NPs: Nanoparticles; ATCC: American Type Culture Collection.

In the case of resistant (MDR) microbial strains, these did not form an inhibition zone around the impregnated microdisks.

When binary dilutions from these types of AgNPs were used on the *S. aureus* ATCC 25923 strain, 1/2 dilution formed an inhibition zone with a diameter of 8.88 mm and an area of 61.9 mm^2, 1/4 dilution formed an inhibition zone with a diameter of 8.29 mm and an area of 53.95 mm^2, 1/8 dilution formed an inhibition zone with a diameter of 7.61 mm and an area of 45.46 mm^2, while 1/16 dilution generated an inhibition zone with a diameter of 7.34 mm and an area of 42.29 mm^2 (Table 2).

The last dilution, 1/32, did not form an inhibition zone around the microdisks impregnated with these amounts of Ag/EG NPs.

Table 2 – ***Diameter and area of the inhibition zone around each microdisk impregnated with 35 μg from each AgNPs (in decreasing dilutions). The analyzed strain was*** **S. aureus** ***ATCC 25923***

***S. aureus* ATCC 25923**							
Dilution		***1/1***	***1/2***	***1/4***	***1/8***	***1/16***	***1/32***
Diameter of the inhibition zone [mm]	*Ag/EG NPs*	10.35	8.88	8.29	7.61	7.34	0
	Ag/EG/PVP NPs	9.79	10.3	9.48	8.83	7.41	0
Area of the inhibition zone [mm^2]	*Ag/EG NPs*	84.09	61.9	53.95	45.46	42.29	0
	Ag/EG/PVP NPs	75.23	83.28	70.55	61.2	43.1	0

Ag: Silver; NPs: Nanoparticles; ATCC: American Type Culture Collection; EG: Ethylene glycol; PVP: Polyvinylpyrrolidone.

Ag/EG/PVP NPs formed the largest inhibition zone on the *C. albicans* ATCC 10231 strain, with a diameter of 13.08 mm and an area of 134.3 mm^2. This was followed by the *S. aureus* ATCC 25923 strain, which formed an inhibition zone with a diameter of 10.26 mm and an area of 82.63 mm^2 (Figure 6b), and the *P. aeruginosa* ATCC 27853 strain, with an inhibition zone that had a diameter of 10.1 mm and an area of 80.07 mm^2. In the case of *E. coli* ATCC 25922 strain, the diameter of the inhibition zone was 9.27 mm and its area was 67.45 mm^2 (Table 3).

Table 3 – ***Diameter and area of the inhibition zone developed by Ag/EG/PVP NPs against the four microbial reference strains***

Reference strain	Diameter of the inhibition zone [mm]	Area of the inhibition zone [mm^2]
S. aureus ATCC 25923	10.26	82.64
E. coli ATCC 25922	9.27	67.45
P. aeruginosa ATCC 27853	10.1	80.07
C. albicans ATCC 10231	13.08	134.3

Ag: Silver; EG: Ethylene glycol; PVP: Polyvinylpyrrolidone; NPs: Nanoparticles; ATCC: American Type Culture Collection.

When these AgNPs were used against resistant (MDR) microbial strains, there was no inhibition zone around the microdisks.

For testing binary dilutions of Ag/EG/PVP NPs on the *S. aureus* ATCC 25923 strain, 1/2 dilution formed an inhibition zone with a diameter of 10.3 mm and an area of 83.28 mm^2, 1/4 dilution formed an inhibition zone with a diameter of 9.48 mm and an area of 70.55 mm^2. The 1/8 dilution formed an inhibition zone with a diameter of 8.83 mm and an area of 61.2 mm^2, while 1/16 dilution formed an inhibition zone with a diameter of 7.41 mm and an area of 43.1 mm^2 (Table 2).

Just as before, the 1/32 diluted NPs did not form an inhibition zone around the microdisks in which they were impregnated.

Table 4 and Figure 7 highlight the comparative view of the area of the inhibition zone developed around each microdisk impregnated with 35 μg from each AgNPs and then placed into culture media containing the four microbial reference strains.

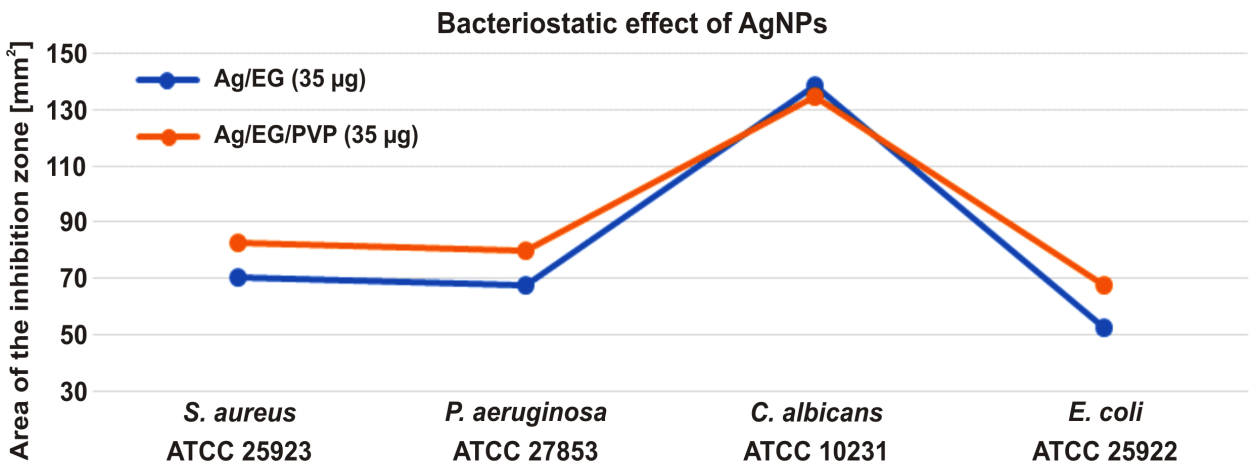

Figure 7 – ***Area of the inhibition zone developed around each microdisk impregnated with 35 µg from each AgNPs and then placed into culture media containing the four microbial reference strains. Ag: Silver; EG: Ethylene glycol; PVP: Polyvinylpyrrolidone; NPs: Nanoparticles; ATCC: American Type Culture Collection.***

Table 4 – ***Comparative view of the area of the inhibition zone developed around each microdisk impregnated with 35 µg from each AgNPs and then placed into culture media containing the four microbial reference strains***

Reference strain	Area of the inhibition zone [mm²]	
	Ag/EG NPs	*Ag/EG/PVP NPs*
S. aureus ATCC 25923	70.55	82.64
P. aeruginosa ATCC 27853	67.75	80.07
C. albicans ATCC 10231	138.2	134.3
E. coli ATCC 25922	52.4	67.45

Ag: Silver; NPs: Nanoparticles; EG: Ethylene glycol; PVP: Polyvinylpyrrolidone; ATCC: American Type Culture Collection.

Discussions

In recent decades, the study of NPs has gained a great scientific interest, due to a wide range of potential applications, in various fields: electronic, optical and biomedical [28–32]. Some of the most studied effects of NPs are antibacterial, as it was shown that many metal NPs have toxic effects on bacterial or viral strains. In addition, the frequent and sometimes incorrect use of antibiotics has created favorable conditions for the selection and development of antibiotic-resistant bacteria, so that today the prevalence of infections with MDR bacteria is growing alarmingly [33, 34].

For these reasons, since 2005, nanomaterials have been extensively studied for possible use in the medical and pharmaceutical fields [32, 35]. Of these, the most intensively investigated are AgNPs that appear to have the ability to inhibit numerous pathogenic bacteria, such as *E. coli*, *P. aeruginosa*, *S. aureus*, etc. [17, 19]; also, it seems that AgNPs have anti-inflammatory and anticancer effects [20, 36].

In our study, starting from $AgNO_3$, we made spherical AgNPs, with a cca. 30 nm diameter, functionalized with EG and PVP. These NPs, at a concentration of 1 mg/mL, were tested in the Laboratory of Microbiology, to determine their antibacterial properties. To prevent agglutination and maintain a homogeneous dispersion in aqueous solution of AgNPs, they were coated with EG or with EG and PVP. It has been shown that the two substances act as stabilizing agents, but also as reducing agents of AgNPs [37–39].

Several studies have shown that the bactericidal activity of AgNPs depends on their size and shape [40–42]. It appears that the spherical AgNPs offer the largest contact surface with bacteria, having the highest bactericidal capacity [43]. Also, other studies have shown that smaller AgNPs exhibit higher bacterial toxicity [31, 44]. In our study, by obtaining cca. 30 nm spherical AgNPs, we believe that we have created optimal conditions for optimal testing of the antibacterial effects of AgNPs.

In our study, we evaluated the antimicrobial effects of AgNPs on known microbial strains (reference strains) but also on antibiotic resistant strains, selected from the pathological products of patients admitted to the Emergency County Hospital, Craiova, Romania, during July–October 2018.

In the diffusimetric method, we used 35 µg of AgNPs for each antibiogram disk, and the dilutions started from 1 mg/mL to 1/32 mg/mL.

Our study confirms the data obtained by other researchers, demonstrating that the bactericidal action of AgNPs varies depending on the concentration of the NPs. Also, the bactericidal activity of AgNPs is variable from one pathogen to another.

The mechanism of bactericidal actions of AgNPs is not well understood and demonstrated to this day. There are several hypotheses that attempt to explain the action of AgNPs. Thus, Sondi & Salopek-Sondi (2004), by electron microscopy studies, show that the bactericidal activity of AgNPs is due to the interaction between them and the constituent elements of the bacterial membrane, through which structural changes occur, and then the deterioration of bacterial membranes eventually leading to cell death [45]. Other studies have shown that the action of AgNPs on the microbial membrane would be due to the Ag^+ ions that bind to the thiol (–SH) groups in the proteins and enzymes found on the surface of the microbial membrane, causing increased cell membrane permeability and altered cellular adenosine triphosphate (ATP) synthesis pathways. Also, AgNPs would cause direct cell membrane injury resulting in the penetration of Ag^+ ions into the cell and their interaction with intracellular

proteins and enzymes containing –SH groups, and even with intracellular organelles (ribosomes), blocking their activity [46–48].

Other studies argue that AgNPs would induce the formation of reactive oxygen species (ROS) that affect metabolic processes and cell division and cause irreversible damage to microbial deoxyribonucleic acid (DNA) [49–51].

Other studies claim that Ag^+ ions are strong nucleic acid binders and form different complexes with DNA or ribonucleic acid (RNA). They preferentially interact with the nitrogenous bases, in particular with guanine and adenine, causing the blocking of bacterial DNA replication [52, 53].

Conclusions

We succeeded in synthesizing and physically characterizing AgNPs, with a diameter of ~30 nm, functionalized with EG and, respectively, with EG and PVP. Tested in microbial cultures, the two types of AgNPs have shown antibacterial effects, varying from one type of germ to another. The most sensitive to the action of the AgNPs was the strain of *C. albicans*, and the least sensitive was *E. coli*. The sensitivity of pathogenic germs was directly proportional to the concentration of AgNPs in the test solution.

Conflict of interests

The authors declare no conflict of interests.

Acknowledgments

This work was supported by a grant of the Romanian Ministry of Research and Innovation, CCDI – UEFISCDI, project number PN-III-P1-1.2-PCCDI-2017-0749/45, within PNCDI III.

References

[1] Shriram V, Khare T, Bhagwat R, Shukla R, Kumar V. Inhibiting bacterial drug efflux pumps *via* phyto-therapeutics to combat threatening antimicrobial resistance. Front Microbiol, 2018, 9:2990.
[2] Dahal RH. Antimicrobial resistance: a major issue in global public health. Clin Biotechnol Microbiol, 2017, 1(5):186–188.
[3] O'Neill J. Antimicrobial resistance: tackling a crisis for the health and wealth of nations. The Review on Antimicrobial Resistance, London, 2014, available at: https://amr-review.org/sites/default/files/AMR%20Review%20Paper%20-%20Tackling%20a%20crisis%20for%20the%20health%20and%20wealth%20of%20nations_1.pdf.
[4] Laxminarayan R, Matsoso P, Pant S, Brower C, Røttingen JA, Klugman K, Davies S. Access to effective antimicrobials: a worldwide challenge. Lancet, 2016, 387(10014):168–175.
[5] Planta MB. The role of poverty in antimicrobial resistance. J Am Board Fam Med, 2007, 20(6):533–539.
[6] Franci G, Falanga A, Galdiero S, Palomba L, Rai M, Morelli G, Galdiero M. Silver nanoparticles as potential antibacterial agents. Molecules, 2015, 20(5):8856–8874.
[7] Gebeyehu E, Bantie L, Azage M. Inappropriate use of antibiotics and its associated factors among urban and rural communities of Bahir Dar City Administration, Northwest Ethiopia. PLoS One, 2015, 10(9):e0138179.
[8] Roy Choudhury S, Goswami A. Supramolecular reactive sulphur nanoparticles: a novel and efficient antimicrobial agent. J Appl Microbiol, 2013, 114(1):1–10.
[9] Herman A, Herman AP. Nanoparticles as antimicrobial agents: their toxicity and mechanisms of action. J Nanosci Nanotechnol, 2014, 14(1):946–957.
[10] Istrate CM, Holban AM, Grumezescu AM, Mogoantă L, Mogoşanu GD, Savopol T, Moisescu M, Iordache M, Vasile BŞ, Kovacs E. Iron oxide nanoparticles modulate the interaction of different antibiotics with cellular membranes. Rom J Morphol Embryol, 2014, 55(3):849–856.
[11] Rădulescu M, Andronescu E, Cirja A, Holban AM, Mogoantă L, Bălşeanu TA, Cătălin B, Neagu TP, Lascăr I, Florea DA, Grumezescu AM, Ciubuca B, Lazăr V, Chifiriuc MC, Bolocan A. Antimicrobial coatings based on zinc oxide and orange oil for improved bioactive wound dressings and other applications. Rom J Morphol Embryol, 2016, 57(1):107–114.
[12] Raghunath A, Perumal E. Metal oxide nanoparticles as antimicrobial agents: a promise for the future. Int J Antimicrob Agents, 2017, 49(2):137–152.
[13] Wang L, Hu C, Shao L. The antimicrobial activity of nanoparticles: present situation and prospects for the future. Int J Nanomedicine, 2017, 12:1227–1249.
[14] Palanisamy NK, Ferina N, Amirulhusni AN, Mohd-Zain Z, Hussaini J, Ping LJ, Durairaj R. Antibiofilm properties of chemically synthesized silver nanoparticles found against *Pseudomonas aeruginosa*. J Nanobiotechnology, 2014, 12:2.
[15] Vazquez-Muñoz R, Avalos-Borja M, Castro-Longoria E. Ultrastructural analysis of *Candida albicans* when exposed to silver nanoparticles. PLoS One, 2014, 9(10):e108876.
[16] Zhang T, Wang L, Chen Q, Chen C. Cytotoxic potential of silver nanoparticles. Yonsei Med J, 2014, 55(2):283–291.
[17] Birla SS, Tiwari VV, Gade AK, Ingle AP, Yadav AP, Rai MK. Fabrication of silver nanoparticles by *Phoma glomerata* and its combined effect against *Escherichia coli*, *Pseudomonas aeruginosa* and *Staphylococcus aureus*. Lett Appl Microbiol, 2009, 48(2):173–179.
[18] Radulescu M, Andronescu E, Dolete G, Popescu RC, Fufă O, Chifiriuc MC, Mogoantă L, Bălşeanu TA, Mogoşanu GD, Grumezescu AM, Holban AM. Silver nanocoatings for reducing the exogenous microbial colonization of wound dressings. Materials (Basel), 2016, 9(5):345.
[19] Dakal TC, Kumar A, Majumdar RS, Yadav V. Mechanistic basis of antimicrobial actions of silver nanoparticles. Front Microbiol, 2016, 7:1831.
[20] Nakkala JR, Mata R, Sadras SR. Green synthesized nano silver: synthesis, physicochemical profiling, antibacterial, anticancer activities and biological *in vivo* toxicity. J Colloid Interface Sci, 2017, 499:33–45.
[21] Amini E, Azadfallah M. *In situ* synthesis of silver nanoparticles on fiber matrix for preparing antibacterial paper. Biointerface Res Appl Chem, 2018, 8(4):3449–3456.
[22] Mahjouri S, Movafeghi A, Divband B, Kosari-Nasab M, Kazemi EM. Assessing the toxicity of silver nanoparticles in cell suspension culture of *Nicotiana tabacum*. Biointerface Res Appl Chem, 2018, 8(3):3252–3258.
[23] Narasaiah BP, Mandal BK, Chakravarthula SN. Mitigation of textile industries generated pollution by agro-waste cotton peels mediated synthesized silver nanoparticles. Biointerface Res Appl Chem, 2018, 8(5):3602–3610.
[24] Sabry NM, Tolba S, Abdel-Gawad FK, Bassem SM, Nassar HF, El-Taweel GE, Okasha A, Ibrahim M. Interaction between nano silver and bacteria: modeling approach. Biointerface Res Appl Chem, 2018, 8(5):3570–3574.
[25] Samoilova NA, Krayukhina MA, Popov DA, Anuchina NM, Piskarev VE. 3'-Sialyllactose-decorated silver nanoparticles: lectin binding and bactericidal properties. Biointerface Res Appl Chem, 2018, 8(1):3095–3099.
[26] Sharma N, Phutela K, Goel A, Soni S, Batra N. Exploring the bacterial based silver nanoparticle for their possible application as disinfectants. Biointerface Res Appl Chem, 2018, 8(1): 3100–3104.
[27] Singh K, Panghal M, Kadyan S, Chaudhary U, Yadav JP. Green silver nanoparticles of *Phyllanthus amarus* as an antibacterial agent against multi drug resistant clinical isolates of *Pseudomonas aeruginosa*. J Nanobiotechnol, 2014, 12:40.
[28] Taylor R, Coulombe S, Otanicar T, Phelan P, Gunawan A, Wei L, Rosengarten G, Prasher R, Tyagi H. Small particles, big impacts: a review of the diverse applications of nanofluids. J Appl Phys, 2013, 113(1):011301.
[29] Holban AM, Grumezescu AM, Gestal MC, Mogoanta L, Mogosanu GD. Novel drug delivery magnetite nano-systems used in antimicrobial therapy. Curr Org Chem, 2014, 18(2): 185–191.
[30] Grumezescu AM, Gestal MC, Holban AM, Grumezescu V, Vasile BS, Mogoantă L, Iordache F, Bleotu C, Mogoşanu GD.

Biocompatible Fe_3O_4 increases the efficacy of amoxicillin delivery against Gram-positive and Gram-negative bacteria. Molecules, 2014, 19(4):5013–5027.
[31] Vimbela GV, Ngo SM, Fraze C, Yang L, Stout DA. Antibacterial properties and toxicity from metallic nanomaterials. Int J Nanomedicine, 2017, 12:3941–3965.
[32] Cheon JY, Lee HM, Park WH. Formation of silver nanoparticles using fluorescence properties of chitosan oligomers. Mar Drugs, 2018, 16(1):11.
[33] Levy SB, Marshall B. Antibacterial resistance worldwide: causes, challenges and responses. Nat Med, 2004, 10(12 Suppl): S122–S129.
[34] Davies J, Davies D. Origins and evolution of antibiotic resistance. Microbiol Mol Biol Rev, 2010, 74(3):417–433.
[35] Kreuter J. Nanoparticles – a historical perspective. Int J Pharm, 2007, 331(1):1–10.
[36] Suwan T, Khongkhunthian S, Sirithunyalug J, Okonogi S. Effect of rice variety and reaction parameters on synthesis and antibacterial activity of silver nanoparticles. Drug Discov Ther, 2018, 12(5):267–274.
[37] Guo G, Gan W, Luo J, Xiang F, Zhang J, Zhou H, Liu H. Preparation and dispersive mechanism of highly dispersive ultrafine silver powder. Appl Surf Sci, 2010, 256(22):6683–6687.
[38] Wu C, Mosher BP, Lyons K, Zeng T. Reducing ability and mechanism for polyvinylpyrrolidone (PVP) in silver nanoparticles synthesis. J Nanosci Nanotechnol, 2010, 10(4):2342–2347.
[39] Dhakal TR, Mishra SR, Glenn Z, Rai BK. Synergistic effect of PVP and PEG on the behavior of silver nanoparticles–polymer composites. J Nanosci Nanotechnol, 2012, 12(8): 6389–6396.
[40] Elechiguerra JL, Burt JL, Morones JR, Camacho-Bragado A, Gao X, Lara HH, Yacaman MJ. Interaction of silver nanoparticles with HIV-1. J Nanobiotechnology, 2005, 3:6.
[41] Morones JR, Elechiguerra JL, Camacho A, Holt K, Kouri JB, Ramírez JT, Yacaman MJ. The bactericidal effect of silver nanoparticles. Nanotechnology, 2005, 16(10):2346–2353.
[42] Pal S, Tak YK, Song JM. Does the antibacterial activity of silver nanoparticles depend on the shape of the nanoparticle? A study of the Gram-negative bacterium *Escherichia coli*. Appl Environ Microbiol, 2007, 73(6):1712–1720.
[43] Priyaragini S, Sathishkumar SR, Bhaskararao KV. Biosynthesis of silver nanoparticles using actinobacteria and evaluating its antimicrobial and cytotoxicity activity. Int J Pharm Pharm Sci, 2013, 5(Suppl 2):709–712.
[44] Chernousova S, Epple M. Silver as antibacterial agent: ion, nanoparticle, and metal. Angew Chem Int Ed Engl, 2013, 52(6):1636–1653.
[45] Sondi I, Salopek-Sondi B. Silver nanoparticles as antimicrobial agent: a case study on *E. coli* as a model for Gram-negative bacteria. J Colloid Interface Sci, 2004, 275(1):177–182.
[46] Yamanaka M, Hara K, Kudo J. Bactericidal actions of silver ion solution on *Escherichia coli*, studied by energy-filtering transmission electron microscopy and proteomic analysis. Appl Environ Microbiol, 2005, 71(11):7589–7593.
[47] Morones-Ramirez JR, Winkler JA, Spina CS, Collins JJ. Silver enhances antibiotic activity against Gram-negative bacteria. Sci Transl Med, 2013, 5(190):190ra81.
[48] Ivask A, Elbadawy A, Kaweeteerawat C, Boren D, Fischer H, Ji Z, Chang CH, Liu R, Tolaymat T, Telesca D, Zink JI, Cohen Y, Holden PA, Godwin HA. Toxicity mechanisms in *Escherichia coli* vary for silver nanoparticles and differ from ionic silver. ACS Nano, 2014, 8(1):374–386.
[49] Feng QL, Wu J, Chen GQ, Cui FZ, Kim TN, Kim JO. A mechanistic study of the antibacterial effect of silver ions on *Escherichia coli* and *Staphylococcus aureus*. J Biomed Mater Res, 2000, 52(4):662–668.
[50] Zhang W, Li Y, Niu J, Chen Y. Photogeneration of reactive oxygen species on uncoated silver, gold, nickel, and silicon nanoparticles and their antibacterial effects. Langmuir, 2013, 29(15):4647–4651.
[51] Agnihotri S, Mukherji S, Mukherji S. Immobilized silver nanoparticles enhance contact killing and show highest efficacy: elucidation of the mechanism of bactericidal action of silver. Nanoscale, 2013, 5(16):7328–7340.
[52] Arakawa H, Neault JF, Tajmir-Riahi HA. Silver(I) complexes with DNA and RNA studied by Fourier transform infrared spectroscopy and capillary electrophoresis. Biophys J, 2001, 81(3):1580–1587.
[53] Barras F, Aussel L, Ezraty B. Silver and antibiotic, new facts to an old story. Antibiotics (Basel), 2018, 7(3):79.

Corresponding author
Cristina Jana Busuioc, Associate Professor, MD, PhD, Department of Histology, University of Medicine and Pharmacy of Craiova, 2 Petru Rareş Street, 200349 Craiova, Dolj County, Romania; Phone +40351–461 458, e-mail: dr_cristinab@yahoo.com

Received: March 15, 2019

Accepted: November 20, 2019